
Budget-Adaptive Adapter Tuning in Orthogonal Subspaces for Continual Learning in LLMs

Zhiyi Wan¹, Wanrou Du¹, Liang Li², Miao Pan³, Xiaoqi Qin¹

¹Beijing University of Posts and Telecommunications

²Pengcheng Laboratory

³University of Houston

{wzy10, wanroudu, xiaoqiqin}@bupt.edu.cn, lil03@pcl.ac.cn, mpan2@uh.edu

Abstract

Large language models (LLMs) often suffer from catastrophic forgetting in continual learning (CL) scenarios, where performance on previously learned tasks degrades severely while training on sequentially arriving tasks. Although pioneering CL approaches using orthogonal subspaces can mitigate task interference, they typically employ fixed budget allocation, neglecting the varying complexity across tasks and layers. Besides, recent budget-adaptive tuning methods for LLMs often adopt multi-stage paradigms that decouple optimization and budget allocation. Such decoupling results in potential misalignment, which hinders those approaches' practical application in CL scenarios. To address these limitations, we propose OA-Adapter, a novel parameter-efficient approach for continual learning in LLMs that unifies dynamic budget adaptation with orthogonal subspace learning in a single end-to-end training stage. Specifically, OA-Adapter introduces a dynamic bottleneck dimension adaptation mechanism that simultaneously allocates an efficient parameter budget and optimizes task objectives without misalignment. To effectively preserve previously acquired knowledge while coordinating with the dynamic budget allocation, orthogonal constraints are applied specifically between the parameter subspace of the current task and the dynamically allocated parameter subspaces of historical tasks. Experimental results on continual learning benchmarks demonstrate that OA-Adapter outperforms state-of-the-art methods in both accuracy and parameter efficiency, achieving higher average accuracy while using 58.5% fewer parameters on the standard CL benchmark.

1 Introduction

Recent advances in large language models (LLMs) have transformed artificial intelligence by demonstrating remarkable capabilities across diverse domains, from text generation to logical reasoning [1, 2]. However, real-world deployment demands that LLMs continually adapt to evolving user needs and emerging tasks while retaining previously acquired knowledge—a prerequisite for sustainable lifelong learning [3, 4].

Parameter-efficient fine-tuning (PEFT) methods, such as adapter modules [5] and low-rank adaptation (LoRA) [6], enable task-specific adaptation by updating only 0.01% – 4% of model weights [7]). While originally designed to reduce computational costs for single-task tuning [8, 9], these methods struggle in continual learning with sequentially arriving tasks. Sequentially tuning to arriving tasks induces catastrophic forgetting-severe degradation of performance on prior tasks [10]. One intuitive solution is to store task-specific adapters for each new task. However, this approach consumes substantial storage resources and leads to considerable inflexibility in multi-task deployments. Alternatively, retraining models with archived historical and additional new data necessitates frequent

model updates and large data repositories [11]. Both strategies are prohibitively costly and impractical in resource-constrained environments.

To efficiently adapt LLMs to downstream tasks while preserving previously acquired knowledge, researchers proposed continual learning (CL) methods, as discussed in Appendix A.1. However, most CL approaches operate within shared parameter spaces across tasks, which inherently induces cross-task interference [12, 11, 13–19]. Furthermore, unlike conventional CL benchmarks that typically handle tasks with limited distribution shifts (e.g., incremental image classification), continual learning for LLMs often deals with substantially divergent task distributions, thus significantly amplifying interference when tuning in shared parameter spaces. Some methods further dynamically construct task-specific parameters for new knowledge integration to resolve this problem, but they heavily rely on explicit task identifiers during inference [20–24].

Recent research efforts in orthogonal subspace learning [25–27] offer a promising alternative by restricting task-specific updates to mutually orthogonal parameter subspaces, decoupling optimization directions across tasks and thereby eliminating interference and task ID dependency. However, existing methods typically rely on a fixed budget allocation, assigning the same subspace dimensionality to every task and layer. This rigid strategy overlooks the heterogeneity of task complexity and layer-specific adaptation needs, leading to inefficient parameter utilization, allocating excessive resource to simple tasks while under-allocating resources to more complex ones. Such inflexible allocation hinders LLMs’ continuous adaptation capabilities in practice.

To achieve dynamic budget allocation, emerging budget-adaptive PEFT methods like AdaLoRA [28], ElaLoRA [29], and DiffoRA [30] proposed multi-stage paradigms with sequential optimization and budget adjustment phases, as detailed in Appendix A.1. Such decoupled optimization may create misalignment between fine-tuning objectives and budget allocation. Moreover, the inherent complexity of multi-stage designs introduces substantial computational overhead and engineering challenges, limiting their practicality for continual learning systems.

To address these issues, we propose OA-Adapter, a novel parameter-efficient approach for continual learning in LLMs. Instead of manually assigning a fixed budget, OA-Adapter automatically adjusts the parameter budget for each task and layer based on the task difficulty and model capacity. To the best of our knowledge, this is the first work to integrate budget adaptation into parameter-efficient fine-tuning for continual learning in LLMs.

Our key contributions are as follows:

- We propose OA-Adapter, a novel parameter-efficient approach for continual learning in LLMs that unifies dynamic budget adaptation with orthogonal subspace learning in a single end-to-end training stage.
- We design a dynamic bottleneck dimension adaptation mechanism that simultaneously allocates an efficient parameter budget and optimizes task objectives without misalignment.
- We establish orthogonal constraints between the parameter subspace of the current task and the dynamically allocated parameter subspaces of historical tasks, effectively preserving previously acquired knowledge while coordinating with the dynamic dimension adaptation.
- Experimental results demonstrate that OA-Adapter outperforms state-of-the-art methods in both accuracy and parameter efficiency. OA-Adapter achieves higher average accuracy with 58.5% fewer parameters on the standard CL benchmark and maintains its advantages on a larger benchmark comprising 15 tasks.

2 Methodology

In this section, we introduce OA-Adapter, a novel framework for continual learning in LLMs that simultaneously improves parameter efficiency and mitigates catastrophic forgetting in a single end-to-end training stage, as illustrated in Fig. 1. We first describe its architectural design, including core components and computation flow. Then, we analyze the mathematical foundations of the dynamic bottleneck dimension adaptation, demonstrating how trainable thresholds enable bidirectional activation and deactivation of dimensions during a single training phase. Finally, we formalize the orthogonal parameter subspace constraints mechanism and explain how it works in concert with the dynamic bottleneck dimension adaptation to achieve parameter-efficient continual learning.

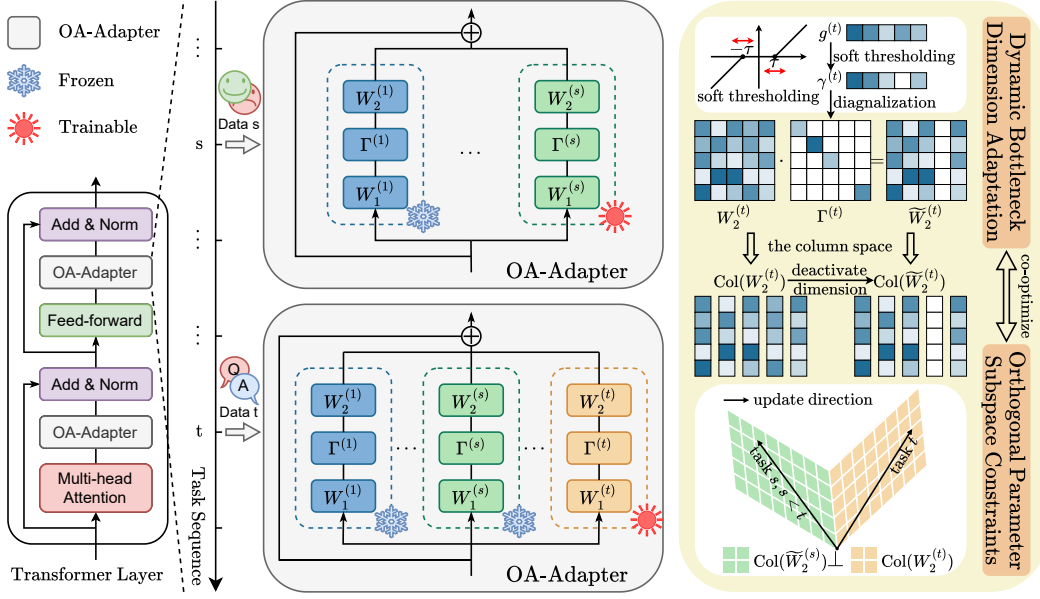


Figure 1: The OA-Adapter framework for LLM continual learning. Each task-specific OA-Adapter module (task t) comprises three core components: (1) a down-projection layer $W_1^{(t)}$, (2) a trainable diagonal mask $\Gamma^{(t)}$ with trainable threshold $\tau^{(t)}$, and (3) an up-projection layer $W_2^{(t)}$. The dynamic masking mechanism enables bidirectional dimension adaptation through activation/deactivation of latent dimensions. Orthogonal subspace constraints are enforced between the column space of the t -th task parameters $\text{Col}(W_2^{(t)})$ and the dynamically allocated parameter subspaces of historical tasks $\text{Col}(\widetilde{W}_2^{(s)})$ (for $s < t$). Here, $\widetilde{W}_2^{(s)}$ incorporates only the activated dimensions from the s -th task.

2.1 Module Structure

Standard Adapter. When adapting pre-trained language models (PLMs) to downstream tasks, traditional full-parameter fine-tuning proves both parameter-inefficient and computationally expensive. To enable efficient adaptation, adapter modules inject lightweight trainable parameters into PLMs while keeping the original weights frozen. These modules employ a bottleneck architecture to minimize trainable parameters, consisting of three layers: 1) a down-projection layer that reduces the original d -dimensional representation x to a lower dimension r , 2) a nonlinear activation function $f(\cdot)$, and 3) an up-projection layer that restores the features to dimension d . The architecture ensures near-zero initialization of the projection layers while maintaining a skip connection to preserve the original features during initial training stages. For an input representation $x \in \mathbb{R}^d$, the adapter’s output $y \in \mathbb{R}^d$ can be formalized as:

$$y = x + W_2 \cdot f(W_1 \cdot x + b_1) + b_2, \quad (1)$$

where $W_1 \in \mathbb{R}^{r \times d}$, $W_2 \in \mathbb{R}^{d \times r}$ denote the down-projection and up-projection matrices. $b_1 \in \mathbb{R}^r$ and $b_2 \in \mathbb{R}^d$ denote the bias terms, respectively, with bottleneck dimension $r \ll d$.

OA-Adapter. Building upon the standard Adapter’s bottleneck architecture, OA-Adapter introduces two structural modifications: 1) the removal of bias terms in projection layers to create a bias-free parameter space containing only linear transformations, and 2) the replacement of static non-linear activations with a trainable diagonal masking matrix Γ that dynamically adjusts the bottleneck dimension, as detailed in Section 2.2. These modifications enable the enforcement of orthogonal parameter subspace constraints, as detailed in Section 2.3, to mitigate cross-task interference and co-optimization of budget adaptation with continual learning in a single training phase. Specifically, the forward computation of OA-Adapter operates as follows:

$$y = x + W_2 \cdot \Gamma \cdot W_1 \cdot x, \quad (2)$$

where $\mathcal{W}_1 \in \mathbb{R}^{r_{\max} \times d}$ and $\mathcal{W}_2 \in \mathbb{R}^{d \times r_{\max}}$ denote the down-projection and up-projection matrices, respectively, and $\Gamma \in \mathbb{R}^{r_{\max} \times r_{\max}}$ is a trainable diagonal masking matrix. Here, $r_{\max} \ll d$ represents the pre-defined maximum bottleneck dimension.

2.2 Dynamic Bottleneck Dimension Adaptation

Adaptation Mechanism. To dynamically allocate parameter budget, we adjust the effective bottleneck dimensions of OA-Adapter using a trainable diagonal masking matrix $\Gamma \in \mathbb{R}^{r_{\max} \times r_{\max}}$: $\Gamma = \text{diag}(\gamma)$. The sparsity of the vector $\gamma \in \mathbb{R}^{r_{\max}}$ is controlled via a soft thresholding mechanism applied to a trainable vector $g \in \mathbb{R}^{r_{\max}}$. Specifically, each diagonal entry γ_i is computed as:

$$\gamma_i = \text{soft}(g_i; \tau) = \text{sign}(g_i) \cdot \max(|g_i| - \tau, 0), \quad (3)$$

where $\tau > 0$ is a trainable threshold that dynamically modulates the sparsity level of Γ throughout the training process. The projection path of OA-Adapter can then be equivalently reformulated as:

$$\mathcal{W}_2 \cdot \Gamma \cdot \mathcal{W}_1 = \sum_{i=1}^{r_{\max}} \gamma_i \cdot \mathcal{W}_2[:, i] \otimes \mathcal{W}_1[i, :], \quad (4)$$

where \otimes denotes the outer product. This decomposition clearly demonstrates how each γ_i dynamically adjusts the contribution of the i^{th} latent dimension pair: when $|g_i| \leq \tau$, we have $\gamma_i = 0$, causing both the i^{th} column of \mathcal{W}_2 and i^{th} row of \mathcal{W}_1 to be disabled, effectively deactivating the corresponding dimension. This mechanism adaptively controls the bottleneck dimension through $r_{\text{eff}} = \|\gamma\|_0$, where $\|\gamma\|_0$ represents the count of non-zero entries in γ .

Gradient Analysis. Our method’s bidirectional dimension adaptation capability, enabled by the trainable threshold τ , offers critical advantages. When $|g_i| \leq \tau$, the corresponding dimension pair is deactivated by setting $\gamma_i = 0$. This zeros the i -th diagonal entry of the masking matrix Γ , effectively removing that dimension’s contribution in forward propagation. However, this operation also blocks gradient flow from the downstream loss \mathcal{L} to g_i when $\gamma_i = 0$. To clarify why g_i becomes non-trainable in such cases, consider the gradient calculation via chain rule:

$$\frac{\partial \mathcal{L}}{\partial g_i} = \frac{\partial \mathcal{L}}{\partial \gamma_i} \frac{\partial \gamma_i}{\partial g_i}. \quad (5)$$

The derivative $\frac{\partial \gamma_i}{\partial g_i}$ of the soft thresholding function equals $\text{sign}(g_i)$ when $|g_i| > \tau$, but critically becomes 0 when $|g_i| \leq \tau$. This implies that deactivated dimensions (where $|g_i| \leq \tau$) produce zero gradients in Equation (5) due to $\frac{\partial \gamma_i}{\partial g_i} = 0$, blocking gradient updates through g_i . With a fixed threshold τ , such dimensions would remain permanently disabled throughout training. Crucially, our method implements τ as a learnable parameter shared across all dimensions within each OA-Adapter module. Thus, the gradient of τ with respect to the total loss \mathcal{L} is derived through chain rule as:

$$\frac{\partial \mathcal{L}}{\partial \tau} = \sum_{i=1}^{r_{\max}} \frac{\partial \mathcal{L}}{\partial \gamma_i} \frac{\partial \gamma_i}{\partial \tau}, \quad (6)$$

where $\frac{\partial \gamma_i}{\partial \tau} = -\text{sign}(g_i)$ when $|g_i| > \tau$ and 0 otherwise. This derivative relationship ensures threshold updates are primarily governed by dimensions exceeding the current τ . As τ evolves during training, dimensions previously deactivated with $|g_i| \leq \tau$ may become reactivated when they satisfy $|g_i| > \tau$ under the updated threshold, thereby reactivating their corresponding projection paths. This bidirectional adaptation mechanism automatically suppresses dimensions while maintaining their potential for reactivation in later training iterations. The bidirectional nature of this dynamic parameter budget adaptation approach ensures optimal parameter allocation that continuously adapts to the evolving requirements of sequential tasks in continual learning.

2.3 Orthogonal Parameter Subspace Constraints for Continual Learning

Continual Learning Setup. Continual learning focuses on incrementally acquiring knowledge from evolving data distributions of sequential tasks while mitigating catastrophic forgetting of previously acquired knowledge. Formally, models are trained on a sequential stream of tasks denoted as $\{D_1, D_2, \dots, D_t\}$. Each task $D_t = (x_t^i, y_t^i)_{i=1}^{n_t}$ consists of input instances $x_t^i \in \mathcal{X}_t$ paired with

corresponding labels $y_t^i \in \mathcal{Y}_t$, where \mathcal{X}_t and \mathcal{Y}_t represent the task-specific input and label spaces. During the training phase for task D_t , model parameters Φ are updated exclusively using data from D_t . The objective of continual learning can be formalized as optimizing:

$$\max_{\Phi} \sum_{t=1}^T \sum_{\{x_t^i, y_t^i\} \in \mathcal{D}_t} \log P_{\Phi}(y_t^i | x_t^i). \quad (7)$$

Orthogonal Parameter Subspace Constraints. Catastrophic forgetting arises when task-specific adaptations overwrite parameters critical for previous tasks. To mitigate this, we introduce orthogonality constraints that enforce parameter updates across tasks to occupy mutually independent subspaces. Let $\Delta\Phi_k = \mathcal{W}_2^{(k)} \Gamma^{(k)} \mathcal{W}_1^{(k)}$ represent the OA-Adapter’s parameter update for the k -th task. We have:

$$\Delta\Phi_k = \widetilde{\mathcal{W}}_2^{(k)} \cdot \mathcal{W}_1^{(k)} = (\mathcal{W}_2^{(k)} \cdot \Gamma^{(k)}) \cdot \mathcal{W}_1^{(k)} \quad (8)$$

Here, the columns of $\widetilde{\mathcal{W}}_2^{(k)}$ serve as orthogonal basis vectors spanning the parameter update subspace for the k -th task, while $\mathcal{W}_1^{(k)}$ determines how these basis vectors are combined. We therefore formally define the task-specific parameter subspace as the column space of $\widetilde{\mathcal{W}}_2^{(k)}$, which intrinsically aligns with the activated dimensions for the k -th task through the dimension-selective masking operation of $\Gamma^{(k)}$. Thus, we enforce strict orthogonality to new OA-Adapter parameters across sequential tasks, ensuring new task adaptations occupy parameter subspaces orthogonal to previous tasks’ frozen parameter subspaces. Formally, the constraints for the t -th task is defined as:

$$\langle \mathcal{W}_2^{(t)}[:, i], \widetilde{\mathcal{W}}_2^{(s)}[:, j] \rangle = 0, \forall i, j, s < t \quad (9)$$

The columns of $\widetilde{\mathcal{W}}_2^{(t)}$ inherit directional properties from $\mathcal{W}_2^{(t)}$, ensuring orthogonal relationships persist regardless of dynamic dimension activation patterns. These asymmetric orthogonality constraints enable simultaneous optimization of dynamic bottleneck dimension adaptation and historical knowledge preservation. To formalize this approach, we incorporate an orthogonality regularization term into the optimization objective. Specifically, the pairwise orthogonality loss between current task t and each historical task $s < t$ is quantified as:

$$\mathcal{L}_{\text{orth}}^{(s,t)} = \sum_{i,j} \left\langle \mathcal{W}_2^{(t)}[:, i], \widetilde{\mathcal{W}}_2^{(s)}[:, j] \right\rangle^2 \quad (10)$$

Minimizing the loss term $\mathcal{L}_{\text{orth}}^{(s,t)}$ drives the inner product $\langle \mathcal{W}_2^{(t)}[:, i], \widetilde{\mathcal{W}}_2^{(s)}[:, j] \rangle$ toward zero, enforcing parameter subspace orthogonality. The complete training objective, integrating both task-specific performance and orthogonality constraints, is formulated as:

$$\mathcal{L}_{\text{total}} = \mathcal{L}_{\text{task}}^{(t)} + \lambda_{\text{orth}} \cdot \sum_{s < t} \mathcal{L}_{\text{orth}}^{(s,t)} \quad (11)$$

where $\mathcal{L}_{\text{task}}^{(t)}$ represents the primary loss for task t , and λ_{orth} is a hyperparameter controlling the strength of orthogonality regularization.

3 Experiments

3.1 Experimental Settings.

Datasets. We evaluate our approach using two CL benchmarks for LLMs. The first is the standard CL benchmark [31], which comprises 5 text classification datasets: AG News, Amazon Reviews, Yelp Reviews, DBpedia, and Yahoo Answers. The second is a continual learning benchmark consisting of a larger number of tasks with 15 datasets [20]. This benchmark includes five tasks from the standard CL benchmark, four from GLUE benchmark (MNLI, QQP, RTE, SST2) [32], five from SuperGLUE benchmark (WiC, CB, COPA, MultiRC, BoolQA) [33] and the IMDB movie reviews dataset [34]. Following the methodology of [20], we randomly select 1000 samples per class for training. The task details and training sequences of tasks used in our experiments are provided in Appendix A.5.

Metrics. Let $a_{i,j}$ denote the test accuracy on the i -th task after training on the j -th task. To evaluate performance, we use the mean accuracy over all tasks after completing training on the final task. Specifically, it is defined as $\frac{1}{T} \sum_{i=1}^T a_{i,T}$, where T is the total number of tasks.

Table 1: Testing performance on two standard CL benchmarks with T5-large.

	Standard CL Benchmark				Large Number of Tasks			
	Order-1	Order-2	Order-3	Average	Order-4	Order-5	Order-6	Average
SeqFT	18.9	24.9	41.7	28.5	7.4	7.4	7.5	7.4
EWC	48.7	47.7	54.5	50.3	45.3	44.5	45.6	45.1
LwF	54.4	53.1	49.6	52.3	50.1	43.1	47.4	46.9
Inc-Adapter	57.5	47.8	66.1	57.1	54.3	46.1	58.1	52.8
Replay	55.2	56.9	61.3	57.8	55.0	54.6	53.1	54.2
L2P	60.3	61.7	61.1	60.7	57.5	53.8	56.9	56.1
LFPT5	68.6	72.4	76.9	72.6	69.4	67.8	68.6	68.6
O-Adapter	73.3	73.4	73.1	73.3	69.3	61.8	65.7	65.6
O-LoRA	75.0	75.4	75.6	75.3	71.2	63.8	70.6	68.7
OA-Adapter	75.7	76.2	76.1	76.0	70.9	65.2	71.4	69.2
ProgPrompt	75.1	75.0	75.2	75.1	78.0	77.7	77.9	77.9
PerTaskFT	70.0	70.0	70.0	70.0	78.1	78.1	78.1	78.1
MTL	80.0	80.0	80.0	80.0	76.5	76.5	76.5	76.5

Baselines. We compare our method against various CL baseline approaches, including: **SeqFT** [35] trains all model parameters on a sequence of tasks without any regularization or replaying samples from the previous tasks. **EWC** [36] finetune the whole model with a regularization loss that prevents updating parameters that could interfere with previously learned tasks. **LwF** [37] constrains the shared representation layer to be similar to its original state before learning the new task. **Inc-Adapter** trains new Adapter parameters on a sequential series of tasks without any constraints or mechanism. **Replay** finetunes the whole model with a memory buffer, and replay samples from old tasks when learning new tasks to avoid forgetting. **L2P** [38] uses the input to dynamically select and update prompts from the prompt pool in an instance-wise fashion. **LFPT5** [39] continuously train a soft prompt that simultaneously learns to solve the tasks and generate training samples, which are subsequently used in experience replay. **O-Adapter** train new Adapter parameters on a sequential series of tasks with orthogonal parameter subspace constraints. **O-LoRA** [27] train new LoRA parameters on a sequential series of tasks in orthogonal subspace while fixing the LoRA matrices of previous tasks. **ProgPrompt** [20] adopts a task-specific soft prompt for each distinct task, sequentially appending it to prior learned prompts. In essence, it trains individual models per task, leveraging the task ID to select the appropriate model during inference. **PerTaskFT** train a separate model for each task. **MTL** train a model simultaneously on all tasks as multi-task learning. This approach represents the theoretical upper bound for continual learning performance with a single model, as it maintains access to the entire task distribution throughout training, thus eliminating the fundamental forgetting challenge in continual learning scenarios. In our continual learning baseline selection, we specifically focused on methods that could be reliably reproduced to ensure fair comparison. Furthermore, to guarantee the authenticity and consistency of our experimental results, we reproduced and reran all baseline methods in our infrastructure.

3.2 Main Results

Our experiments employ the encoder-decoder T5 model [40], consistent with baselines in CL for NLP. Following previous works [39, 27], we report the results of three independent runs with different task orders on each CL benchmark, in Tab.1. All experimental results are reported as the average of three runs. For more detailed settings, refer to Appendix A.4.

Results on Standard Continual Learning Benchmarks. Across all task orders of the standard CL benchmark, OA-Adapter consistently surpasses previous methods by a significant margin, as illustrated in Table 1. Notably, OA-Adapter, compared to the prior state-of-the-art method O-LoRA, achieves performance closer to MTL, the upper bound of continual learning with a single model. Additionally, the performance demonstrates a clear descending trend from OA-Adapter to O-Adapter to Inc-Adapter, providing intuitive evidence that orthogonal parameter subspace constraints effectively prevent catastrophic forgetting, while dynamic bottleneck dimension adaptation further enhances performance through efficient budget allocation. Furthermore, our approach significantly outperforms

PerTaskFT, which indicates that OA-Adapter not only avoids catastrophic forgetting but also utilizes knowledge from prior tasks to enhance the learning of new tasks.

Performance with Large Number of Tasks. On the more challenging benchmark comprising 15 tasks, OA-Adapter consistently outperforms O-LoRA, as illustrated in Table 1. While ProgPrompt shows higher accuracy, it requires task identifiers during inference and maintains separate parameters per task, fundamentally limiting its generalization to unseen tasks and practical deployment in real-world LLM applications. Notably, all continual learning methods still trail behind PerTaskFT and MTL, highlighting that continual learning for a large number of tasks remains a significant challenge.

Parameter Efficiency Analysis. As established in Section 2.2, OA-Adapter leverages dynamic parameter budget allocation to achieve enhanced parameter efficiency. To quantify this advantage, we compare the parameter utilization between OA-Adapter and O-LoRA across various initial budget conditions, as illustrated in Table 2. For OA-Adapter, budget allocation represents bottleneck dimension distribution, while for O-LoRA, it determines the module’s intrinsic rank. Remarkably, OA-Adapter achieves superior performance while using 46.6% to 58.5% fewer parameters compared to O-LoRA’s fixed budget approach. Moreover, OA-Adapter maintains consistent performance excellence across all tested initial budget settings, demonstrating its robust dynamic allocation capabilities. These results highlight our method’s ability to effectively adapt parameter budget allocation according to task-specific requirements, providing substantial efficiency benefits over static parameter budget allocation approaches.

Table 2: Comparisons of parameter efficiency between OA-Adapter and O-LoRA.

Initial Budget	Method	Avg Final Budget	Params	Avg Performance
16	O-LoRA	16	4.72M	75.3
	OA-Adapter	9.95	1.96M-58.5%	76.0+0.7
8	O-LoRA	8	2.36M	74.5
	OA-Adapter	6.05	1.18M-50.0%	74.7+0.2
4	O-LoRA	4	1.18M	73.8
	OA-Adapter	3.18	0.63M-46.6%	74.1+0.3

3.3 Discussions

Occurrence and Mitigation of Catastrophic Forgetting. We first demonstrate the occurrence and mitigation of catastrophic forgetting over Order-1 on the standard CL benchmark. As shown in Figure 2, we observe a significant decline of each task after their training phase without orthogonal parameter subspace constraints. Performance on Task 2 deteriorates to nearly zero by the end of the subsequent two tasks, while performance on Task 1 and Task 3 significantly decreases from their respective levels at the end of their training phases. In contrast, the performance with orthogonal parameter subspace constraints remains largely preserved by the end of Task 4, with the most severe degradation limited to only 14% performance loss on Task 2. These results demonstrate that severe forgetting phenomena occur during multi-task training and confirm that orthogonal parameter subspace constraints can effectively and consistently mitigate such forgetting. Similar trends are consistently observed under other task orders, as detailed in Appendix A.2.

Additionally, as expected, each task achieves higher performance more rapidly during its corresponding training phase without orthogonal subspace constraints, though the final performance is not substantially higher than with orthogonal parameter subspace constraints. This occurs because the model has greater flexibility in parameter update directions when not constrained to preserve previous knowledge, thus more easily finding optimal solutions. Meanwhile, this also demonstrates that while orthogonal subspace constraints limit the model’s choice of update directions, they still maintain sufficient capacity for subsequent tasks.

Interestingly, tasks exhibit brief performance recovery at the beginning of subsequent training phases before experiencing extended forgetting. Performance on Task 1 recovers to nearly 100% at the start of Task 3 and to approximately 60% during Task 4. Despite performance on Task 2 declining to near-zero by the end of Task 3, it shows rapid improvement during initial Task 4 training. The phenomenon resembles human memory: knowledge seemingly forgotten from disuse often requires

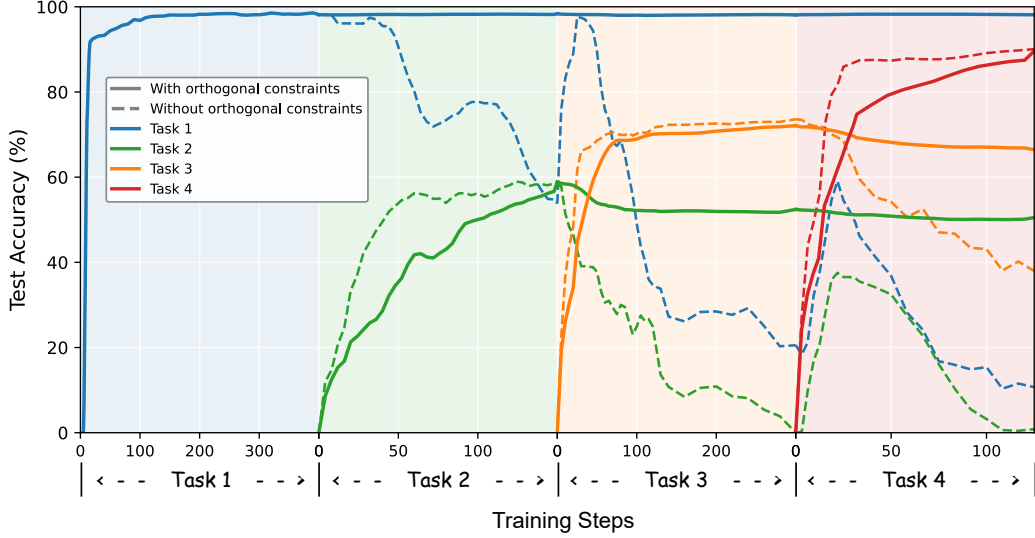


Figure 2: Occurrence and mitigation of catastrophic forgetting during sequential training following Order-1 across multiple tasks. Solid lines represent models with orthogonal parameter subspace constraints, while dashed lines indicate models without. Each color corresponds to a specific task’s test accuracy. Colored background shading denotes the training phase for each respective task, with the X-axis scaled proportionally to accommodate varying training step durations.

minimal effort to reactivate. This suggests that apparent catastrophic forgetting merely masks a latent recovery potential within the model, indicating that knowledge representations remain partially preserved despite significant performance degradation.

Heterogeneous Budget Requirements Across Tasks and Layers. Intuitively, adapting to individual downstream datasets requires varying parameter budgets across different tasks and layers. To validate this, we analyze budget allocation patterns in CL scenarios, as shown in Figure 3. Our results reveal heterogeneous budget requirements across tasks and layer positions, confirming that optimal parameter allocation cannot follow uniform rules but demands task-specific consideration. Notably, in CL scenarios, the parameter matrices for the initial task exhibit significantly higher sparsity compared to subsequent tasks. This pattern supports our hypothesis that initial tasks primarily leverage capabilities inherent in the pretrained model, while later tasks must additionally preserve knowledge from preceding tasks, necessitating more complex parameter spaces. Comprehensive analysis is provided in Appendix A.3. These findings validate the necessity of adaptive budget allocation for CL based on the characteristics of layer, task and training sequence.

Budget Adaptation Mechanism Analysis. To assess the impact of our threshold strategy, we compare two policies: (a) a fixed, non-learnable threshold and (b) our proposed learnable threshold that adapts across different layers and tasks during training, as described in Section 2.2. These strategies are assessed using the T5-large model across three task orders on the standard continual learning benchmark. The results, depicted in Tab. 3, reveal that the dynamic threshold consistently demonstrates superior performance compared to the fixed threshold. This confirms our analysis in Section 2.2, where we demonstrate that the dynamic threshold mechanism enables bidirectional adjustment of budget allocation without introducing complex mechanisms or additional computational overhead, thereby enhancing flexibility in the optimization process.

Pre-trained Model Analysis. We investigate the performance of models across varying model scales (T5-base, T5-large, T5-XL) using the standard continual learning benchmark. We evaluate both our method and O-LoRA across three task orders. The results, depicted in Tab. 4, reveal that OA-Adapter’s average accuracy consistently improves as the parameter size increases, which suggests that our approach effectively leverages the increased representational capacity of larger models. The consistent superiority across different scales indicates that OA-Adapter’s mechanism provides

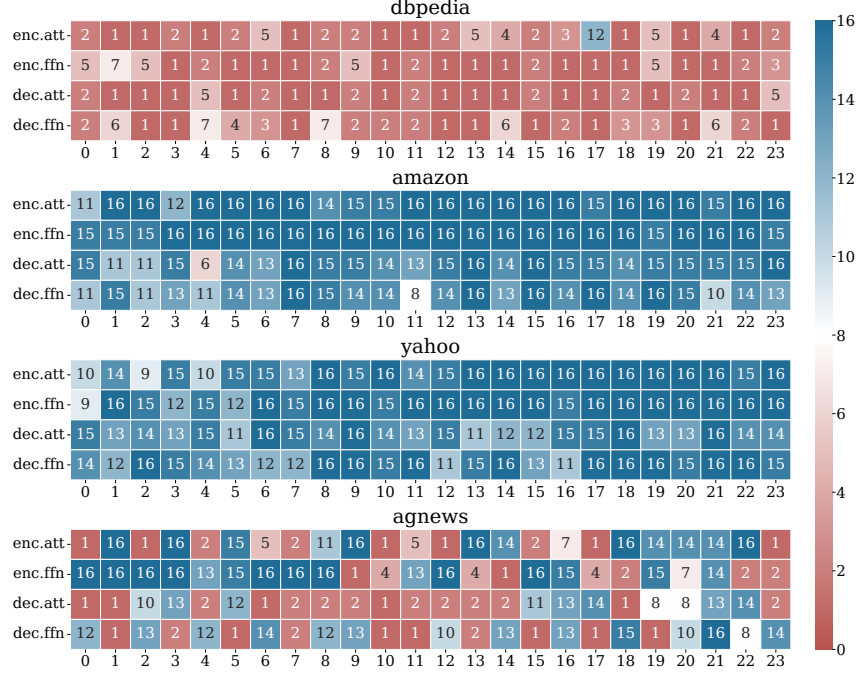


Figure 3: Final dimensions after sequential training following Order-1 with OA-Adapter across four text classification datasets (i.e., DBpedia, Amazon, Yahoo, AG News). The X-axis is the index of T5-large layers, and the Y-axis indicates different layers OA-Adapter applies to.

Table 3: Comparisons of threshold strategies.

Initial Value	Threshold Strategy	order			
		1	2	3	avg
1e-3	fixed	71.5	71.1	71.4	71.3
	dynamic	73.0	76.4	74.6	74.7
1e-4	fixed	73.7	73.1	71.4	72.7
	dynamic	75.7	75.6	75.1	75.5
1e-5	fixed	72.8	73.5	72.3	72.9
	dynamic	74.8	74.9	73.9	74.5

Table 4: Comparisons of model scales.

Model	Method	order			
		1	2	3	avg
T5-base	O-LoRA	73.9	74.8	74.1	74.3
	OA-Adapter	74.7	74.8	74.5	74.7
T5-large	O-LoRA	75.0	75.4	75.6	75.3
	OA-Adapter	75.7	76.2	76.1	76.0
T5-XL	O-LoRA	77.9	78.5	77.4	77.9
	OA-Adapter	78.0	78.2	77.9	78.0

effective protection against catastrophic forgetting while enabling precise task-specific optimization, regardless of the underlying model architecture’s complexity. Moreover, OA-Adapter consistently outperforms O-LoRA across all model scales.

4 Conclusion

In this paper, we introduce OA-Adapter, a novel parameter-efficient approach for continual learning in LLMs that considers both dynamic budget adaptation and orthogonal subspace learning in a single end-to-end training stage. Our comprehensive experiments demonstrate OA-Adapter’s consistent superiority over existing methods across multiple benchmarks while using significantly fewer parameters. The observed heterogeneity in optimal parameter allocation across tasks and layers validates the necessity of our budget-adaptive approach. As the first work to integrate budget adaptation into parameter-efficient fine-tuning for continual learning in LLMs, OA-Adapter establishes a new paradigm that jointly optimizes parameter budget allocation and knowledge preservation. This advancement paves the way for more scalable, efficient, and effective adaptation of LLMs to evolving real-world applications.

References

- [1] D. Zhou, H. Sun, J. Ning, H. Ye, and D. Zhan, “Continual learning with pre-trained models: A survey,” in *Proceedings of the Thirty-Third International Joint Conference on Artificial Intelligence, IJCAI 2024, Jeju, South Korea, August 3-9, 2024*. ijcai.org, 2024, pp. 8363–8371. [Online]. Available: <https://www.ijcai.org/proceedings/2024/924>
- [2] H. Touvron, T. Lavril, G. Izacard, X. Martinet, M. Lachaux, T. Lacroix, B. Rozière, N. Goyal, E. Hambro, F. Azhar, A. Rodriguez, A. Joulin, E. Grave, and G. Lample, “Llama: Open and efficient foundation language models,” *CoRR*, vol. abs/2302.13971, 2023. [Online]. Available: <https://doi.org/10.48550/arXiv.2302.13971>
- [3] Z. Xi, W. Chen, X. Guo, W. He, Y. Ding, B. Hong, M. Zhang, J. Wang, S. Jin, E. Zhou, R. Zheng, X. Fan, X. Wang, L. Xiong, Y. Zhou, W. Wang, C. Jiang, Y. Zou, X. Liu, Z. Yin, S. Dou, R. Weng, W. Qin, Y. Zheng, X. Qiu, X. Huang, Q. Zhang, and T. Gui, “The rise and potential of large language model based agents: a survey,” *Sci. China Inf. Sci.*, vol. 68, no. 2, 2025. [Online]. Available: <https://doi.org/10.1007/s11432-024-4222-0>
- [4] X. Wang, Y. Zhang, T. Chen, S. Gao, S. Jin, X. Yang, Z. Xi, R. Zheng, Y. Zou, T. Gui, Q. Zhang, and X. Huang, “TRACE: A comprehensive benchmark for continual learning in large language models,” *CoRR*, vol. abs/2310.06762, 2023. [Online]. Available: <https://doi.org/10.48550/arXiv.2310.06762>
- [5] N. Houlsby, A. Giurghi, S. Jastrzebski, B. Morrone, Q. de Laroussilhe, A. Gesmundo, M. Attariyan, and S. Gelly, “Parameter-efficient transfer learning for NLP,” in *Proceedings of the 36th International Conference on Machine Learning, ICML 2019, 9-15 June 2019, Long Beach, California, USA*, ser. Proceedings of Machine Learning Research, K. Chaudhuri and R. Salakhutdinov, Eds., vol. 97. PMLR, 2019, pp. 2790–2799. [Online]. Available: <http://proceedings.mlr.press/v97/houlsby19a.html>
- [6] E. J. Hu, Y. Shen, P. Wallis, Z. Allen-Zhu, Y. Li, S. Wang, L. Wang, and W. Chen, “Lora: Low-rank adaptation of large language models,” in *The Tenth International Conference on Learning Representations, ICLR 2022, Virtual Event, April 25-29, 2022*. OpenReview.net, 2022. [Online]. Available: <https://openreview.net/forum?id=nZeVKeeFYf9>
- [7] C. C. S. Balne, S. Bhaduri, T. Roy, V. Jain, and A. Chadha, “Parameter efficient fine tuning: A comprehensive analysis across applications,” *CoRR*, vol. abs/2404.13506, 2024. [Online]. Available: <https://doi.org/10.48550/arXiv.2404.13506>
- [8] X. Zhou, J. He, Y. Ke, G. Zhu, V. Gutiérrez-Basulto, and J. Z. Pan, “An empirical study on parameter-efficient fine-tuning for multimodal large language models,” in *Findings of the Association for Computational Linguistics, ACL 2024, Bangkok, Thailand and virtual meeting, August 11-16, 2024*, L. Ku, A. Martins, and V. Srikumar, Eds. Association for Computational Linguistics, 2024, pp. 10 057–10 084. [Online]. Available: <https://doi.org/10.18653/v1/2024.findings-acl.598>
- [9] Z. Chen, Z. Liu, K. Wang, and S. Lian, “Reparameterization-based parameter-efficient fine-tuning methods for large language models: A systematic survey,” in *Natural Language Processing and Chinese Computing - 13th National CCF Conference, NLPCC 2024, Hangzhou, China, November 1-3, 2024, Proceedings, Part III*, ser. Lecture Notes in Computer Science, D. F. Wong, Z. Wei, and M. Yang, Eds., vol. 15361. Springer, 2024, pp. 107–118. [Online]. Available: https://doi.org/10.1007/978-981-97-9437-9_9
- [10] M. McCloskey and N. J. Cohen, “Catastrophic interference in connectionist networks: The sequential learning problem,” in *Psychology of learning and motivation*. Elsevier, 1989, vol. 24, pp. 109–165.
- [11] H. Shi, Z. Xu, H. Wang, W. Qin, W. Wang, Y. Wang, and H. Wang, “Continual learning of large language models: A comprehensive survey,” *CoRR*, vol. abs/2404.16789, 2024. [Online]. Available: <https://doi.org/10.48550/arXiv.2404.16789>
- [12] L. Wang, X. Zhang, H. Su, and J. Zhu, “A comprehensive survey of continual learning: Theory, method and application,” *IEEE Trans. Pattern Anal. Mach. Intell.*, vol. 46, no. 8, pp. 5362–5383, 2024. [Online]. Available: <https://doi.org/10.1109/TPAMI.2024.3367329>
- [13] A. Chaudhry, M. Rohrbach, M. Elhoseiny, T. Ajanthan, P. K. Dokania, P. H. Torr, and M. Ranzato, “On tiny episodic memories in continual learning,” *arXiv preprint arXiv:1902.10486*, 2019.
- [14] H. Shi and H. Wang, “A unified approach to domain incremental learning with memory: Theory and algorithm,” in *Advances in Neural Information Processing Systems 36: Annual Conference on Neural Information Processing Systems 2023, NeurIPS 2023, New Orleans, LA, USA, December 10 - 16, 2023*, A. Oh, T. Naumann, A. Globerson, K. Saenko, M. Hardt, and S. Levine, Eds., 2023. [Online]. Available: http://papers.nips.cc/paper_files/paper/2023/hash/30d046e94d7b8037d6ef27c4357a8dd4-Abstract-Conference.html

- [15] S. Rebuffi, A. Kolesnikov, G. Sperl, and C. H. Lampert, “icarl: Incremental classifier and representation learning,” in *2017 IEEE Conference on Computer Vision and Pattern Recognition, CVPR 2017, Honolulu, HI, USA, July 21-26, 2017*. IEEE Computer Society, 2017, pp. 5533–5542. [Online]. Available: <https://doi.org/10.1109/CVPR.2017.587>
- [16] R. Aljundi, F. Babiloni, M. Elhoseiny, M. Rohrbach, and T. Tuytelaars, “Memory aware synapses: Learning what (not) to forget,” in *Computer Vision - ECCV 2018 - 15th European Conference, Munich, Germany, September 8-14, 2018, Proceedings, Part III*, ser. Lecture Notes in Computer Science, V. Ferrari, M. Hebert, C. Sminchisescu, and Y. Weiss, Eds., vol. 11207. Springer, 2018, pp. 144–161. [Online]. Available: https://doi.org/10.1007/978-3-030-01219-9_9
- [17] J. Schwarz, W. Czarnecki, J. Luketina, A. Grabska-Barwinska, Y. W. Teh, R. Pascanu, and R. Hadsell, “Progress & compress: A scalable framework for continual learning,” in *Proceedings of the 35th International Conference on Machine Learning, ICML 2018, Stockholmsmässan, Stockholm, Sweden, July 10-15, 2018*, ser. Proceedings of Machine Learning Research, J. G. Dy and A. Krause, Eds., vol. 80. PMLR, 2018, pp. 4535–4544. [Online]. Available: <http://proceedings.mlr.press/v80/schwarz18a.html>
- [18] S. Rongali, A. Jagannatha, B. P. S. Rawat, and H. Yu, “Continual domain-tuning for pretrained language models,” *arXiv preprint arXiv:2004.02288*, 2020.
- [19] G. Lin, H. Chu, and H. Lai, “Towards better plasticity-stability trade-off in incremental learning: A simple linear connector,” in *IEEE/CVF Conference on Computer Vision and Pattern Recognition, CVPR 2022, New Orleans, LA, USA, June 18-24, 2022*. IEEE, 2022, pp. 89–98. [Online]. Available: <https://doi.org/10.1109/CVPR52688.2022.00019>
- [20] A. Razdaibiedina, Y. Mao, R. Hou, M. Khabsa, M. Lewis, and A. Almahairi, “Progressive prompts: Continual learning for language models,” in *The Eleventh International Conference on Learning Representations, ICLR 2023, Kigali, Rwanda, May 1-5, 2023*. OpenReview.net, 2023. [Online]. Available: https://openreview.net/forum?id=UJTgQBc91_
- [21] J. Jang, S. Ye, S. Yang, J. Shin, J. Han, G. Kim, S. J. Choi, and M. Seo, “Towards continual knowledge learning of language models,” in *The Tenth International Conference on Learning Representations, ICLR 2022, Virtual Event, April 25-29, 2022*. OpenReview.net, 2022. [Online]. Available: <https://openreview.net/forum?id=vfsRB5Mlmo9>
- [22] X. Jin, D. Zhang, H. Zhu, W. Xiao, S. Li, X. Wei, A. O. Arnold, and X. Ren, “Lifelong pretraining: Continually adapting language models to emerging corpora,” in *Proceedings of the 2022 Conference of the North American Chapter of the Association for Computational Linguistics: Human Language Technologies, NAACL 2022, Seattle, WA, United States, July 10-15, 2022*, M. Carpuat, M. de Marneffe, and I. V. M. Ruíz, Eds. Association for Computational Linguistics, 2022, pp. 4764–4780. [Online]. Available: <https://doi.org/10.18653/v1/2022.naacl-main.351>
- [23] C. Li and H. Lee, “Examining forgetting in continual pre-training of aligned large language models,” *CoRR*, vol. abs/2401.03129, 2024. [Online]. Available: <https://doi.org/10.48550/arXiv.2401.03129>
- [24] Y. Yan, K. Xue, X. Shi, Q. Ye, J. Liu, and T. Ruan, “AF adapter: Continual pretraining for building chinese biomedical language model,” in *IEEE International Conference on Bioinformatics and Biomedicine, BIBM 2023, Istanbul, Turkiye, December 5-8, 2023*, X. Jiang, H. Wang, R. Alhajj, X. Hu, F. Engel, M. Mahmud, N. Pisanti, X. Cui, and H. Song, Eds. IEEE, 2023, pp. 953–957. [Online]. Available: <https://doi.org/10.1109/BIBM58861.2023.10385733>
- [25] M. Farajtabar, N. Azizan, A. Mott, and A. Li, “Orthogonal gradient descent for continual learning,” in *The 23rd International Conference on Artificial Intelligence and Statistics, AISTATS 2020, 26-28 August 2020, Online [Palermo, Sicily, Italy]*, ser. Proceedings of Machine Learning Research, S. Chiappa and R. Calandra, Eds., vol. 108. PMLR, 2020, pp. 3762–3773. [Online]. Available: <http://proceedings.mlr.press/v108/farajtabar20a.html>
- [26] Y. Guo, W. Hu, D. Zhao, and B. Liu, “Adaptive orthogonal projection for batch and online continual learning,” in *Thirty-Sixth AAAI Conference on Artificial Intelligence, AAAI 2022, Thirty-Fourth Conference on Innovative Applications of Artificial Intelligence, IAAI 2022, The Twelveth Symposium on Educational Advances in Artificial Intelligence, EAAI 2022 Virtual Event, February 22 - March 1, 2022*. AAAI Press, 2022, pp. 6783–6791. [Online]. Available: <https://doi.org/10.1609/aaai.v36i6.20634>
- [27] X. Wang, T. Chen, Q. Ge, H. Xia, R. Bao, R. Zheng, Q. Zhang, T. Gui, and X. Huang, “Orthogonal subspace learning for language model continual learning,” in *Findings of the Association for Computational Linguistics: EMNLP 2023, Singapore, December 6-10, 2023*, H. Bouamor, J. Pino, and K. Bali, Eds. Association for Computational Linguistics, 2023, pp. 10 658–10 671. [Online]. Available: <https://doi.org/10.18653/v1/2023.findings-emnlp.715>

- [28] Q. Zhang, M. Chen, A. Bukharin, N. Karampatziakis, P. He, Y. Cheng, W. Chen, and T. Zhao, “Adalora: Adaptive budget allocation for parameter-efficient fine-tuning,” 2023. [Online]. Available: <https://arxiv.org/abs/2303.10512>
- [29] H. Chang, Z. Ma, M. Ma, Z. Qi, A. Sabot, H. Jiang, and H. Kung, “Elalora: Elastic & learnable low-rank adaptation for efficient model fine-tuning,” *arXiv preprint arXiv:2504.00254*, 2025.
- [30] T. Jiang, H. Wang, and C. Yuan, “Diffora: Enabling parameter-efficient LLM fine-tuning via differential low-rank matrix adaptation,” *CoRR*, vol. abs/2502.08905, 2025. [Online]. Available: <https://doi.org/10.48550/arXiv.2502.08905>
- [31] X. Zhang, J. J. Zhao, and Y. LeCun, “Character-level convolutional networks for text classification,” in *Advances in Neural Information Processing Systems 28: Annual Conference on Neural Information Processing Systems 2015, December 7-12, 2015, Montreal, Quebec, Canada*, C. Cortes, N. D. Lawrence, D. D. Lee, M. Sugiyama, and R. Garnett, Eds., 2015, pp. 649–657. [Online]. Available: <https://proceedings.neurips.cc/paper/2015/hash/250cf8b51c773f3f8dc8b4be867a9a02-Abstract.html>
- [32] A. Wang, A. Singh, J. Michael, F. Hill, O. Levy, and S. R. Bowman, “GLUE: A multi-task benchmark and analysis platform for natural language understanding,” in *7th International Conference on Learning Representations, ICLR 2019, New Orleans, LA, USA, May 6-9, 2019*. OpenReview.net, 2019. [Online]. Available: <https://openreview.net/forum?id=rJ4km2R5t7>
- [33] A. Wang, Y. Pruksachatkun, N. Nangia, A. Singh, J. Michael, F. Hill, O. Levy, and S. Bowman, “Super-glue: A stickier benchmark for general-purpose language understanding systems,” *Advances in neural information processing systems*, vol. 32, 2019.
- [34] A. L. Maas, R. E. Daly, P. T. Pham, D. Huang, A. Y. Ng, and C. Potts, “Learning word vectors for sentiment analysis,” in *The 49th Annual Meeting of the Association for Computational Linguistics: Human Language Technologies, Proceedings of the Conference, 19-24 June, 2011, Portland, Oregon, USA*, D. Lin, Y. Matsumoto, and R. Mihalcea, Eds. The Association for Computer Linguistics, 2011, pp. 142–150. [Online]. Available: <https://aclanthology.org/P11-1015/>
- [35] C. de Masson d’Autume, S. Ruder, L. Kong, and D. Yogatama, “Episodic memory in lifelong language learning,” in *Advances in Neural Information Processing Systems 32: Annual Conference on Neural Information Processing Systems 2019, NeurIPS 2019, December 8-14, 2019, Vancouver, BC, Canada*, H. M. Wallach, H. Larochelle, A. Beygelzimer, F. d’Alché-Buc, E. B. Fox, and R. Garnett, Eds., 2019, pp. 13 122–13 131. [Online]. Available: <https://proceedings.neurips.cc/paper/2019/hash/f8d2e80c1458ea2501f98a2cafadb397-Abstract.html>
- [36] J. Kirkpatrick, R. Pascanu, N. Rabinowitz, J. Veness, G. Desjardins, A. A. Rusu, K. Milan, J. Quan, T. Ramalho, A. Grabska-Barwinska *et al.*, “Overcoming catastrophic forgetting in neural networks,” *Proceedings of the national academy of sciences*, vol. 114, no. 13, pp. 3521–3526, 2017.
- [37] Z. Li and D. Hoiem, “Learning without forgetting,” *IEEE Trans. Pattern Anal. Mach. Intell.*, vol. 40, no. 12, pp. 2935–2947, 2018. [Online]. Available: <https://doi.org/10.1109/TPAMI.2017.2773081>
- [38] Z. Wang, Z. Zhang, C. Lee, H. Zhang, R. Sun, X. Ren, G. Su, V. Perot, J. G. Dy, and T. Pfister, “Learning to prompt for continual learning,” in *IEEE/CVF Conference on Computer Vision and Pattern Recognition, CVPR 2022, New Orleans, LA, USA, June 18-24, 2022*. IEEE, 2022, pp. 139–149. [Online]. Available: <https://doi.org/10.1109/CVPR52688.2022.00024>
- [39] C. Qin and S. Joty, “Lfpt5: A unified framework for lifelong few-shot language learning based on prompt tuning of t5,” *arXiv preprint arXiv:2110.07298*, 2021.
- [40] C. Raffel, N. Shazeer, A. Roberts, K. Lee, S. Narang, M. Matena, Y. Zhou, W. Li, and P. J. Liu, “Exploring the limits of transfer learning with a unified text-to-text transformer,” *J. Mach. Learn. Res.*, vol. 21, pp. 140:1–140:67, 2020. [Online]. Available: <https://jmlr.org/papers/v21/20-074.html>
- [41] Z. Liu, J. Lyn, W. Zhu, X. Tian, and Y. Graham, “ALoRA: Allocating low-rank adaptation for fine-tuning large language models,” in *Proceedings of the 2024 Conference of the North American Chapter of the Association for Computational Linguistics: Human Language Technologies (Volume 1: Long Papers)*, K. Duh, H. Gomez, and S. Bethard, Eds. Mexico City, Mexico: Association for Computational Linguistics, Jun. 2024, pp. 622–641. [Online]. Available: <https://aclanthology.org/2024.naacl-long.35/>
- [42] N. Ding, X. Lv, Q. Wang, Y. Chen, B. Zhou, Z. Liu, and M. Sun, “Sparse low-rank adaptation of pre-trained language models,” in *Proceedings of the 2023 Conference on Empirical Methods in Natural Language Processing*, H. Bouamor, J. Pino, and K. Bali, Eds. Singapore: Association for Computational Linguistics, Dec. 2023, pp. 4133–4145. [Online]. Available: <https://aclanthology.org/2023.emnlp-main.252/>

- [43] D. Rao, F. Visin, A. A. Rusu, R. Pascanu, Y. W. Teh, and R. Hadsell, “Continual unsupervised representation learning,” in *Advances in Neural Information Processing Systems 32: Annual Conference on Neural Information Processing Systems 2019, NeurIPS 2019, December 8-14, 2019, Vancouver, BC, Canada*, H. M. Wallach, H. Larochelle, A. Beygelzimer, F. d’Alché-Buc, E. B. Fox, and R. Garnett, Eds., 2019, pp. 7645–7655. [Online]. Available: <https://proceedings.neurips.cc/paper/2019/hash/861578d797aeb0634f77aff3f488cca2-Abstract.html>

A Appendix

A.1 Related Work.

Continual Learning for LLMs. Existing continual learning (CL) techniques can be broadly classified into several categories, including replay-based, regularization-based, architecture-based, optimization-based, and representation-based methods [12, 11]. Among these, replay-based, regularization-based, and architecture-based methods have been most extensively applied in the context of continual learning for LLMs. Replay-based methods [13–15] maintain a memory buffer containing data from previous tasks, which is used to retrain the model alongside new data. While these methods are valued for their simplicity, stability, and strong performance, their core operation—storing and replaying data—introduces significant privacy concerns and leads to substantial storage overheads, especially given that language datasets often contain personal or sensitive information. Regularization-based methods [16–19] introduce a regularization term that penalizes significant weight deviations across tasks, thereby attempting to balance performance between old and new tasks. However, the complexity of these methods increases rapidly as the number of tasks grows, which often results in a sharp decline in performance retention on older tasks. These approaches primarily focus on learning all incremental tasks within a shared parameter space, which is a major contributor to task interference. In contrast, many architecture-based methods [20–24] address this challenge by proposing incorporating task-specific components, isolated parameters, or dedicated pathways within the model. These strategies essentially learn task-specific expert modules for different tasks. While these methods can effectively mitigate task interference, they often rely heavily on explicit task ID during the inference stage, which limits their ability to generalize across different tasks. Building on a similar principle, recent advancements have explored a promising direction that can retain generalization capacity while reducing task interference without requiring explicit task ID. These methods, such as OGD [25], AOP [26], and O-LoRA [27], constrain weight updates for each task to lie within mutually orthogonal subspaces of the high-dimensional parameter space. By doing so, these methods effectively decouple the optimization directions of different tasks, thereby mitigating interference and preserving performance on previously learned tasks. However, a common limitation of many existing orthogonal subspace methods is that they typically adopt a fixed budget for all tasks and layers. This uniform treatment overlooks the inherent variability in complexity and importance across different tasks and network layers, which is particularly pronounced in large LLMs. To fully exploit the potential of methods based on orthogonal subspace learning, it is essential to develop mechanisms that can dynamically adapt budget allocation based on task-specific and layer-specific requirements.

Adaptive Budget Tuning. Although existing budget-adaptive tuning methods for LLMs differ in implementation details, they commonly adopt a multi-stage design in which budget adaptation is handled in a separate stage from model optimization. This multi-stage paradigm is often designed to identify optimal configurations for different tasks or layers in large-scale models. For example, DiffoRA [30] trains a LoRA module for each layer in the first stage, and then selects a subset of these modules based on a learned Difference-aware Adaptive Matrix in a subsequent stage. ElaLoRA [29] involves a “Warm-up” fine-tuning stage, followed by a “Dynamic Rank Adjustment” stage to adapt LoRA module ranks, and finally a “Stabilization” fine-tuning stage. AdaLoRA [28] injects rank pruning operations after training iterations by applying singular value decomposition (SVD) to selectively retain low-rank components. While these methods achieve strong performance on single-task static datasets, their multi-stage design introduces substantial computational and engineering overhead that compromises practicality and scalability, while creating misalignment between optimization objectives and budget adaptation criteria that ultimately hinders the achievement of truly optimal solutions. Moreover, their design is limited to only unidirectional rank reduction operations, which precludes bidirectional budget adaptation. These characteristics make it particularly challenging to extend such methods to the CL setting, where the training process must be efficient, unified, and adaptive to sequentially arriving tasks. Additionally, recent methods such as ALoRA [41] and ElaLoRA [29] eliminate parameters based on specific importance metrics. While these approaches offer strong interpretability, their elimination ratios rely on empirical settings rather than adapting to the intrinsic differences between sequentially arriving tasks. Imitating the formulation of AdaLoRA, SoRA [42] introduces a proximal gradient-based update rule with strong theoretical grounding. However, it relies on fixed hyperparameters to decide the fixed sparsity threshold, which renders optimization challenging. Furthermore, SoRA’s scheduling algorithm for sparsity indicators is more

suitable for exploring the balance between performance and parameter efficiency after convergence in single-task scenarios, rather than capturing task sequence characteristics in multi-task environments.

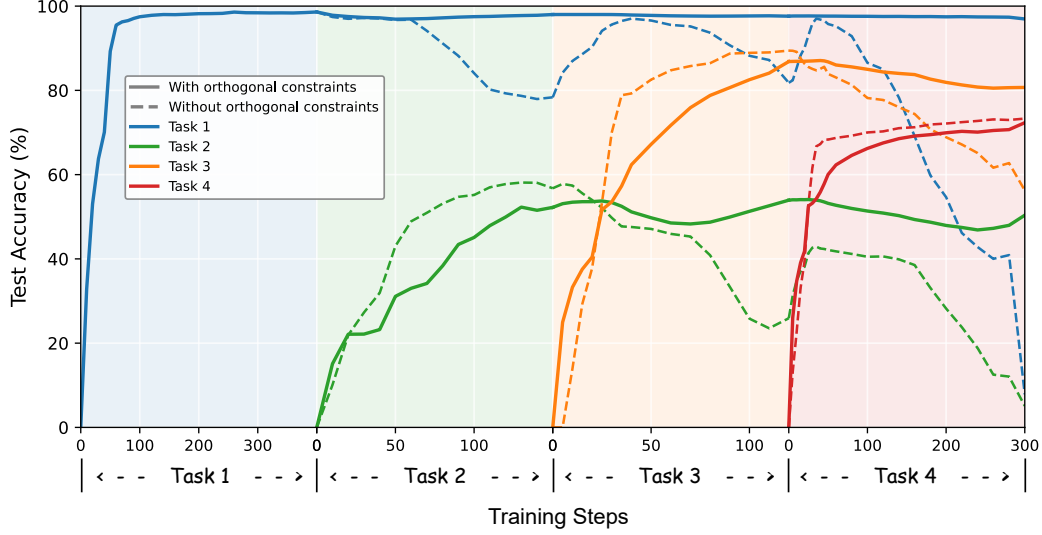


Figure 4: Occurrence and mitigation of catastrophic forgetting during sequential training following Order-2 across multiple tasks.

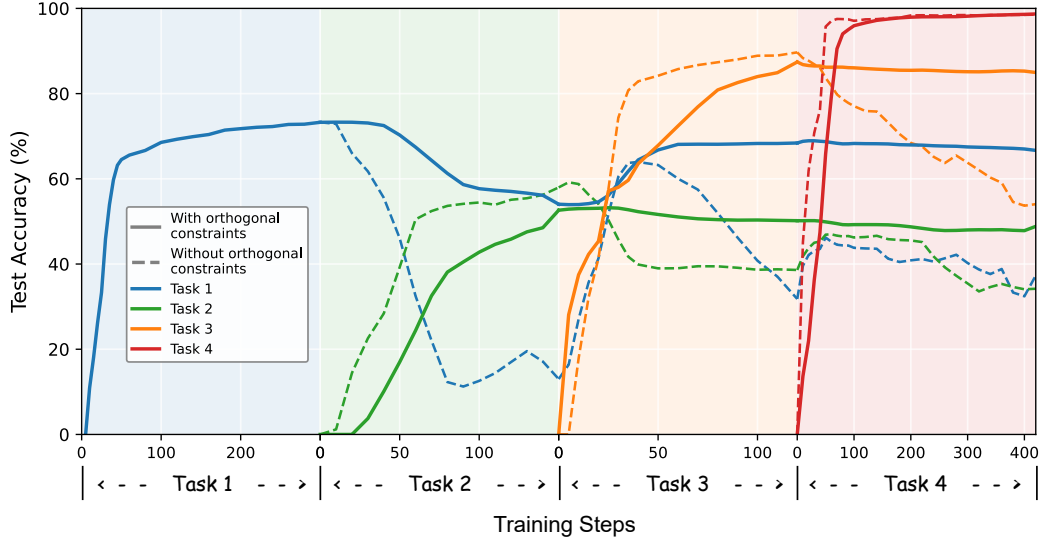


Figure 5: Occurrence and mitigation of catastrophic forgetting during sequential training following Order-3 across multiple tasks.

A.2 Occurrence and Mitigation of Catastrophic forgetting.

To further validate the effectiveness and consistency of orthogonal parameter subspace constraints, we conduct sequential training following Order-2 and Order-3, with results illustrated in Figure 4 and 5, respectively. Consistent with the results reported in Section 3.3, we observe severe catastrophic forgetting in the absence of orthogonal constraints, especially for earlier tasks. In contrast, models trained with orthogonal parameter subspace constraints are able to preserve performance across all tasks to a much greater extent. Notably, although the specific tasks affected most by forgetting vary depending on the task order, the general trend holds: orthogonal constraints provide consistent

mitigation of forgetting regardless of task permutation. These results reinforce our earlier findings and highlight the robustness of orthogonal subspace regularization as a general mechanism for alleviating forgetting in continual learning scenarios.

A.3 Heterogeneous Budget Requirements Across Tasks and Layers.

As discussed in Section 3.3, we extend our analysis to investigate budget allocation in the context of continual learning. Here, we further present results under other task orders, as illustrated in Figure 6 and 7. These findings corroborate our analysis in Section 3.3: (a) The relationship between performance and parameter budget does not follow constant rules but rather necessitates case-specific consideration. (b) Within continual learning scenarios, the first task primarily focuses on acquiring capabilities built upon the pretrained model, whereas subsequent tasks must additionally preserve knowledge from preceding tasks, thus requiring more nuanced fine-tuning. This further substantiates our analysis that different tasks in the CL scenarios require varying budgets, and that allocating budgets according to training sequence and task characteristics is both necessary and justified.

A.4 Implementation Detail.

All our experiments involving T5 models were performed on a server outfitted with four NVIDIA GeForce RTX 3090 GPUs, utilizing the DeepSpeed repository for implementation. Following previous studies [35, 43], for CL experiments, for each dataset we use the available validation set as a test set (since test data is not available) and hold out 500 samples from the train set to construct the validation set. For every sequence of tasks across different orders, we trained the models for one epoch using a batch size of 32 (8 per GPU), a dropout rate of 0.1, and no weight decay. Across all experiments, we primarily used Adapter modules with a bottleneck dimension of 16, and applied a sparsification threshold chosen from $\{1e-3, 1e-4, 1e-5\}$. The learning rate was selected from $\{5e-3, 3e-3, 1e-3, 5e-4\}$ depending on task characteristics. We applied an orthogonality regularization on the Adapter’s upsampling matrix with a coefficient $\lambda_{orth} \in \{0.5, 1, 5\}$, and used an additional coefficient $\lambda_2 \in \{0, 0.1, 0.5\}$ to scale the associated L2 loss term. This flexible configuration allowed us to balance knowledge retention and model sparsity across tasks, especially in long sequences with substantial distribution shifts. To ensure experimental comparability and fair result comparison, we maintain consistency with O-LoRA [27] by adopting instruction tuning as the training paradigm across all experiments for both our method and other baselines, as shown in Table 5. This approach offers dual advantages: it incorporates human expertise for efficient learning while enabling models to better capture underlying principles through explicit guidance, thereby enhancing generalization capabilities. The consistent instruction-based framework allows for direct performance comparisons while leveraging the benefits of natural language supervision.

Table 5: Instructions for different tasks.

Task	Prompts
NLI	What is the logical relationship between the "sentence 1" and the "sentence 2"? Choose one from the option.
QQP	Whether the "first sentence" and the "second sentence" have the same meaning? Choose one from the option.
SC	What is the sentiment of the following paragraph? Choose one from the option.
TC	What is the topic of the following paragraph? Choose one from the option.
BoolQA	According to the following passage, is the question true or false? Choose one from the option.
MultiRC	According to the following passage and question, is the candidate answer true or false? Choose one from the option.
WiC	Given a word and two sentences, whether the word is used with the same sense in both sentence? Choose one from the option.

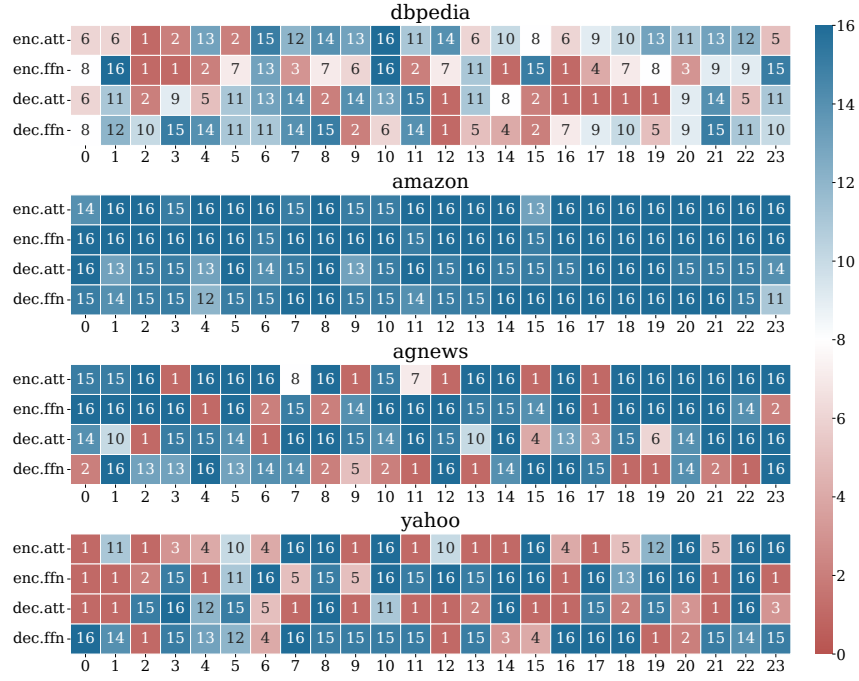


Figure 6: Final dimensions after sequential training following Order-2 with OA-Adapter.

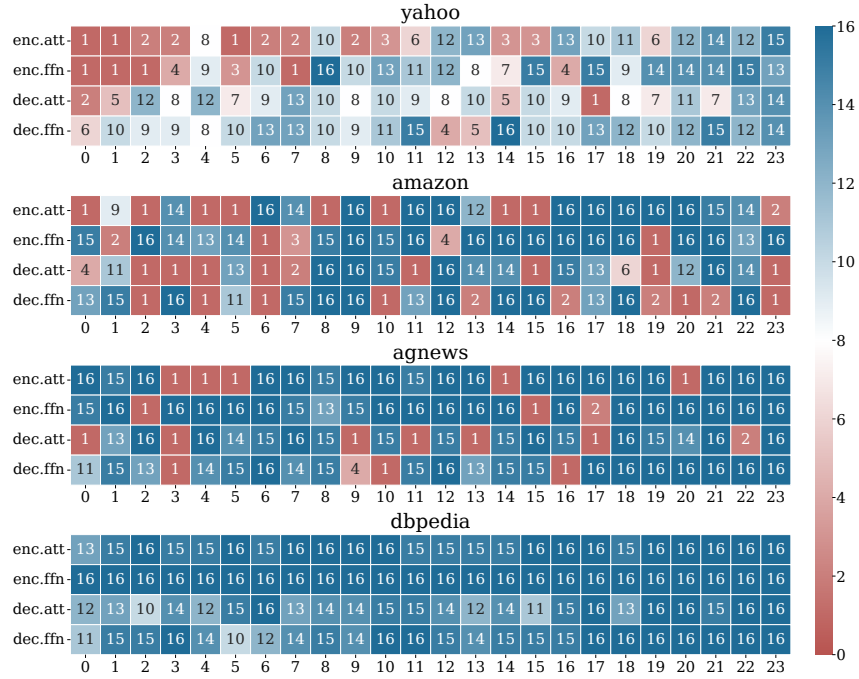


Figure 7: Final dimensions after sequential training following Order-3 with OA-Adapter.

A.5 Datasets and Task Orders.

Table 6 shows details of the 15 datasets we used for our CL experiments, along with their evaluation metrics. Overall, we used datasets from CL benchmark [31], GLUE [32] and SuperGLUE [33] benchmarks, and added IMDB movie reviews dataset [34], following [20]. Table 7 shows details of task orders used for our CL experiments.

Table 6: The details of 15 datasets used in our CL experiments. NLI denotes natural language inference, QA denotes questions and answers task. The first five tasks correspond to the standard CL benchmark, all other tasks are used in long-sequence experiments.

Dataset	Category	Task	Domain	Metric
Yelp	CL Benchmark	Sentiment Analysis	Yelp Reviews	Accuracy
Amazon	CL Benchmark	Sentiment Analysis	Amazon Reviews	Accuracy
DBPedia	CL Benchmark	Topic Classification	Wikipedia	Accuracy
Yahoo	CL Benchmark	Topic Classification	Yahoo Q&A	Accuracy
AG News	CL Benchmark	Topic Classification	News	Accuracy
MNLI	GLUE	NLI	Various	Accuracy
QQP	GLUE	Paraphrase Detection	Quora	Accuracy
RTE	GLUE	NLI	News, Wikipedia	Accuracy
SST-2	GLUE	Sentiment Analysis	Movie Reviews	Accuracy
WIC	SuperGLUE	Word Sense Disambiguation	Lexical Databases	Accuracy
CB	SuperGLUE	NLI	Various	Accuracy
COPA	SuperGLUE	QA	Blogs, Encyclopedia	Accuracy
BoolQA	SuperGLUE	Boolean QA	Wikipedia	Accuracy
MultiRC	SuperGLUE	QA	Various	Accuracy
IMDB	SuperGLUE	Sentiment Analysis	Movie Reviews	Accuracy

Table 7: Six different task sequence orders utilized in continual learning experiments. Orders 1-3 follow the standard continual learning benchmark as established by previous research, focusing on a more traditional task sequence. Orders 4-6 customized for long-sequence experimentation, encompass 15 tasks each and are structured according to the methodologies outlined in [20].

Order	Task Sequence
1	dbpedia → amazon → yahoo → ag
2	dbpedia → amazon → ag → yahoo
3	yahoo → amazon → ag → dbpedia
4	mnli → cb → wic → copa → qqp → boolqa → rte → imdb → yelp → amazon → sst-2 → dbpedia → ag → multirc → yahoo
5	multirc → boolqa → wic → mnli → cb → copa → qqp → rte → imdb → sst-2 → yelp → amazon → ag → dbpedia → yahoo
6	yelp → amazon → mnli → cb → copa → qqp → rte → imdb → sst-2 → dbpedia → ag → yahoo → multirc → boolqa → wic

A.6 Limitations and Further Research Directions.

While our method has demonstrated effectiveness in empirical evaluations, there are a few limitations and potential directions of research to consider. Firstly, although our method does not rely on task identification during inference, it still requires task identification during training. Exploring methods for task-agnostic training would be a valuable future direction. Additionally, while our findings in Figure 2 reveal that models do not completely forget knowledge from previous tasks due to cross-task interference, the underlying mechanisms and potential ways to leverage this phenomenon remain unexplored in our current approach. This represents a promising new perspective and direction for future continual learning research that warrants further investigation.